Documentation for Mill Data Set

Kai Goebel (NASA Ames) & Alice Agogino (UC Berkeley)

The data in this set represents experiments from runs on a milling machine under various operating conditions. In particular, tool wear was investigated (Goebel, 1996) in a regular cut as well as entry cut and exit cut. Data sampled by three different types of sensors (acoustic emission sensor, vibration sensor, current sensor) were acquired at several positions.

The data is organized in a 1x167 matlab struct array with fields as shown in Table 1 below:

Table 1: Struct field names and description

Field name	Description
case	Case number (1-16)
run	Counter for experimental runs in each case
VB	Flank wear, measured after runs; Measurements for VB were not taken after each run
time	Duration of experiment (restarts for each case)
DOC	Depth of cut (does not vary for each case)
feed	Feed (does not vary for each case)
material	Material (does not vary for each case)
smcAC	AC spindle motor current
smcDC	DC spindle motor current
vib_table	Table vibration
vib_spindle	Spindle vibration
AE_table	Acoustic emission at table
AE_spindle	Acoustic emission at spindle

刀具磨损

There are 16 cases with varying number of runs. The number of runs was dependent on the degree of flank wear that was measured between runs at irregular intervals up to a wear limit (and sometimes beyond). Flank wear was not always measured and at times when no measurements were taken, no entry was made.

The 16 cases are enumerated in Table 2

Table 2: Experimental conditions

Case	Depth of Cut	Feed	Material
1	1.5	0.5	1 – cast iron
2	0.75	0.5	1 – case iron
3	0.75	0.25	1 – cast iron
4	1.5	0.25	1 – cast iron
5	1.5	0.5	2 – steel
6	1.5	0.25	2 – steel
7	0.75	0.25	2 – steel
8	0.75	0.5	2 – steel
9	1.5	0.5	1 – cast iron
10	1.5	0.25	1 – cast iron
11	0.75	0.25	1 – cast iron
12	0.75	0.5	1 – cast iron
13	0.75	0.25	2 – steel

14	0.75	0.5	2 – steel
15	1.5	0.25	2 – steel
16	1.5	0.5	2 – steel

Experimental Setup

The setup of the experiment is as depicted in Figure 1 below.

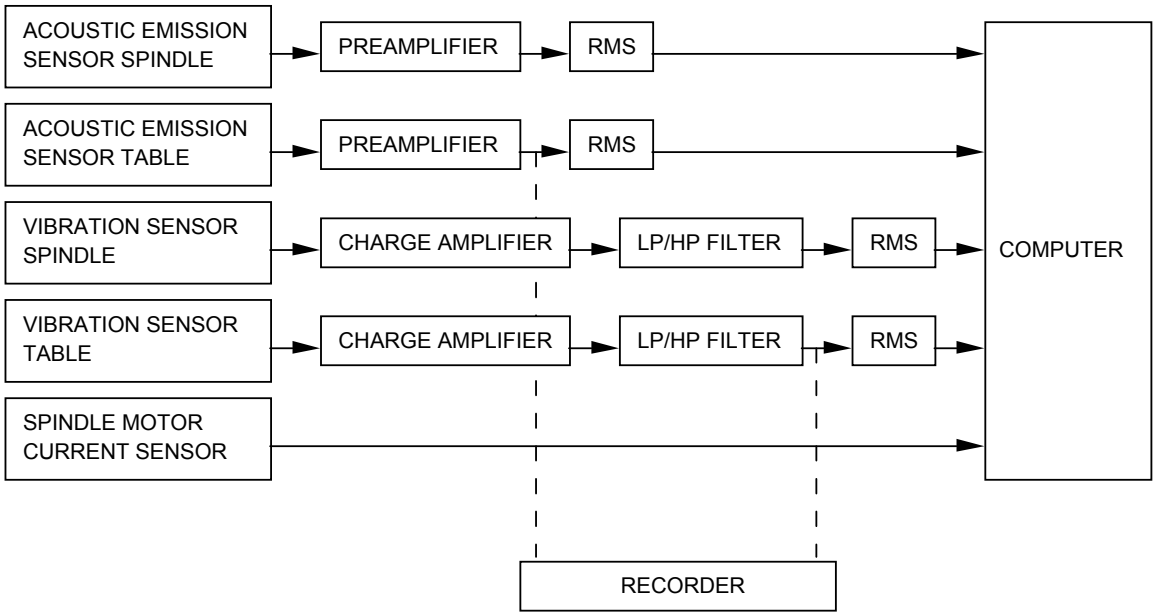

Figure 1 - Experimental Setup

The basic setup encompasses the spindle and the table of the Matsuura machining center MC-510V. An acoustic emission sensor and a vibration sensor are each mounted to the table and the spindle of the machining center. The signals from all sensors are amplified and filtered, then fed through two RMS before they enter the computer for data acquisition. The signal from a spindle motor current sensor is fed into the computer without further processing.

The matrix for the parameters chosen for the experiments were guided by industrial applicability and recommended manufacturer's settings. Therefore, the cutting speed was set to 200 m/min which is equivalent to 826 rev/min. Two different depths of cut were chosen, 1.5mm and 0.75mm. Also, two feeds were taken, 0.5mm/rev and 0.25mm/rev which translate into 413mm/min and 206.5mm/min, respectively. Two types of material, cast iron and stainless steel J45 were used and, as already mentioned earlier, with an inserts of type KC710. These choices equal 8 different settings. All experiments were done a second time with the same parameters with a second set of inserts. The size of the workpieces was 483mm x 178mm x 51mm.

Data Acquisition and Processing

As described in the previous section, the data were sent through a high speed data acquisition board with maximal sampling rate of 100 KHz. The sampled output of the data was used for the signal processing software. LabVIEW® (National Instruments, USA) was used for this task. This software is a general purpose programming development system which uses a graphical language (G). With G, programs are

created in block diagram form. The chosen layout allowed for data acquisition, storage, presentation, and processing. Data were stored to allow for real time simulation and also later analysis.

Several sensor signals underwent preprocessing. In most cases, the signal was amplified to be able to meet threshold requirements of equipment. In particular, the signals from the acoustic emission sensors and from the vibration sensors were amplified to be in the range of ±5V for maximum load, considering the maximum allowable range of the equipment. The signals were filtered by a high pass filter, the vibration sensor signals were additionally filtered with a low pass filter. Corner frequencies were chosen according to the noise that could be observed on an oscilloscope. Periodical noise of 180Hz was observed on the oscilloscope for the vibration signal corresponding to the third harmonic of the main power supply. Therefore, the chosen corner frequency for the low pass filter was 400Hz. For the high pass filter, 1kHz was chosen. Above 8KHz, the range of the acoustic emission sensor ends. That is, readings above that frequency cannot be attributed to any occurrence in the machining process. Since it clutters the signal unnecessarily, it was filtered out. Acoustic emission and vibration signals were fed through an RMS device. Its use smoothes the signal and makes it more accessible to signal processing. The RMS is proportional to the energy contents of the signal, according to the formula:

$$\mathrm{RMS} = \sqrt{\frac{1}{\Delta T}\int_0^{\Delta T} f^2(t)dt}$$

where:

ΔT = time constant

$f(t)$ = signal function

The sampling rate has to be smaller than the time constant to ensure proper data sampling. The chosen parameters were:

ΔT = 8.00ms

sampling rate: 250Hz

Apart from the preprocessed data, raw data of the acoustic emission of the table and the vibration of the table were recorded on a tape recorder to allow for future comparison and evaluation. It might be of interest for feature extraction to have data that did not undergo previous selection; in the same spirit, it is worthwhile to be able to use data that are not “corrupted” yet for neural network techniques or data clustering algorithms. Typical sensor readings from spindle motor current AC and DC portion, acoustic emission at the table, vibration at the table, acoustic emission at the spindle, and vibration at the spindle are displayed in Figure 7 - Figure 12 in the appendix

Detailed Setup Description

Mounted to the table is an acoustic emission sensor model WD 925 (PHYSICAL ACOUSTIC GROUP, frequency range up to 2MHz). The acoustic emission sensor is glued to a custom made base which in turn is attached to the clamping support. The layout of the sensors on the clamping device is shown in Figure 2.

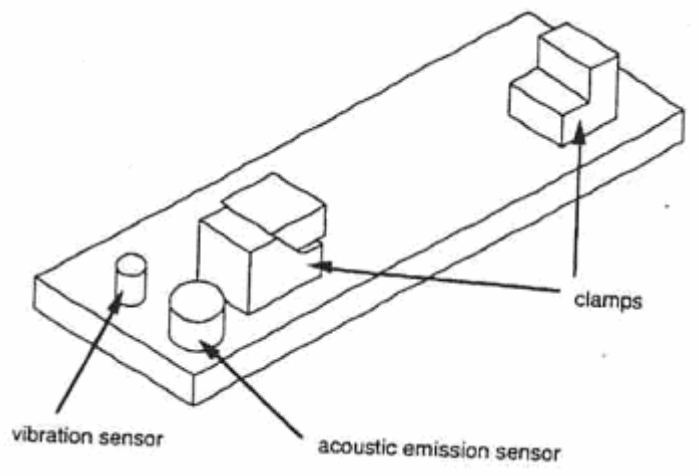

Figure 2 - Clamping device with mounted sensors

The signal from the acoustic emission sensor goes into the single ended terminal of an acoustic emission preamplifier (DUNEGAN/ENDEVCO, model 1801 with integrated 50KHZ high pass filter). The signal is then amplified by a dual amplifier DE model 302A (DUNEGAN/ENDEVCO). The signal is then fed into the RMS meter which is a custom made device built by the LMA of the University of California at Berkeley. The time constant is set to 8.0ms. The signal is then fed into the PHOENIX CONTACT UMK-SE 11,25 cable which feeds the signal into a MIO-16 high speed data acquisition board (National Instruments). The data acquisition board is mounted in a IBM PC 486DX/2-66.

Also mounted on the clamping device on the table is a vibration sensor, an accelerometer (model 7201-50, ENDEVCO) with a frequency range up to 13KHz. Its signal is fed into an ENDEVCO 104 charge amplifier with sensitivity 5.71 and 100mV/g output. The signal is then fed into an ITHACO 4302 DUAL 24dB/octave filter with corner frequencies 400 Hz and 1KHz. Following is a RMS meter same make and settings as described earlier. The signal is then fed then through the PHOENIX CONTACT UMK-SE 11,25 cable connector into the high speed data acquisition board of the computer.

The same vibration sensor that is mounted on the table is also attached to the spindle into a preexisting threaded hole close to the tool. The signal follows the same path as described for the other vibration sensor except that the signal is fed into the PHOENIX CONTACT cable connector.

Signals from another acoustic emission sensor mounted into another threaded hole on the spindle next to the tool is fed into the differential terminal of an acoustic emission preamplifier model 1801 (DUNEGAN/ENDEVCO) and then follows the same path as outlined for the other acoustic emission sensor.

A OMRON K3TB-A1015 current converter, powered by a HP 6237B triple output power supply providing 15V, feeds the signal from one spindle motor current phase into the cable connector.

A model CTA 213 current sensor (Flexcore Div. of Marlan & Associates, Inc.) which uses the same phase of the spindle motor current is fed into the cable connector.

Terminals 33 (ground) and 38 (+5V) are used with a switch to trigger the data acquisition.

With industrial applicability in mind, a 70mm face mill with 6 inserts (Figure 3) was chosen as the tool. The inserts KC710 was selected based on the recommendations for roughing (Kennametal, 1985). KC710 is coated with multiple layers of titanium carbide, titanium carbonitride, and titanium nitride (TiC/TiC-N/TiN) in sequence. These layers retain the toughness of tungsten carbide but have improved resistance to cratering and edge wear. At the same time, they have the advantage of titanium carbide plus reduced face friction. This insert is recommended for heavy roughing.

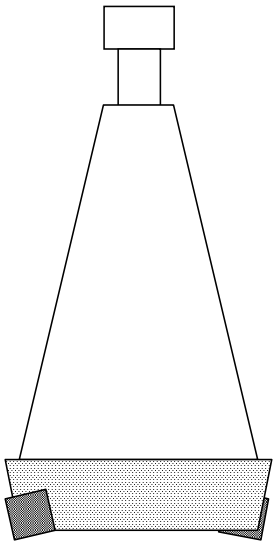

Figure 3 - Schematic of tool and inserts of face mill

The Cutting Process

The interaction of work piece and tool is rather complex and creates a manifold of physical effects, some of which can be captured with sensors. During the engagement of the tool in the work piece, plastic deformation takes place in the shear zone and a chip is formed. Energy is released which results in the radiation of heat, cutting forces, vibration and acoustic emission. Sensors will be used to capture the latter three; they will be explained in more detail.

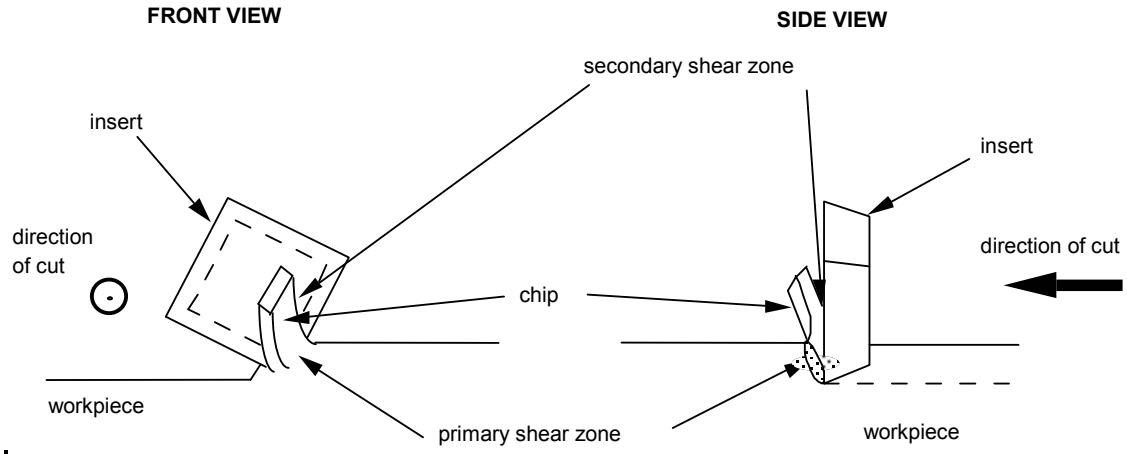

Figure 4 - Shear zones at tool/workpiece interface

Acoustic emission is a high frequency oscillation which occurs spontaneously within metals when they are deformed or fractured. It is caused by the release of strain energy as the micro structure of the material is rearranged. Acoustic emission is generated in the shear zones (Figure 4), the primary as well

as the secondary along the chip/tool interface through bulk deformation and sliding, respectively, and, lastly, at the tool flank/workpiece interface due to friction (Schey, 1977). Although the basic signal of the acoustic emission is sinusoidal, it acquires a random pattern due to reflection and scattering due to structural defects. The range of the oscillation lies between 50kHz and several MHz. Because the signal becomes weaker with increasing distance from the cutting zone, it is desirable to place an acoustic emission sensor close to the cutting process which produces problems of properly protecting the sensor.
Vibration emission is a low frequency oscillation due to the acceleration of the object because of the dynamic changes of cutting forces resulting from periodical changes in tool geometry, chip formation, and built up edges. The range of the signal is 0-40kHz. As with acoustic emission, the vibration sensor should be placed close to the cutting zone because the signal gets weaker with increasing distance from its source. Because the Matsuura machining center is very rigid, vibrations will be significantly lower than in the experiments made on the upright Bridgeport milling machine. However, they still contribute to tool wear and hence have to be taken into consideration.

Cutting forces appear in the primary and secondary shear zone where plastic deformation takes place. Friction between chip and tool and work piece and tool also contribute to cutting forces. Sensors measuring the cutting forces can capture the force directly and indirectly. The direct method requires the installation of force sensors under the work piece which can be cumbersome and costly. The indirect method can measure the deflection of machine parts, motor current of spindle motor or feed motors, and power consumption of spindle or feed motors. Since the spindle motor current is proportional to the torque which in turn is proportional to the cutting force, using this signal is an easy way to capture the force signal. Although perhaps not as accurate as the direct measurement, it is a relatively cheap way and the sensor is easy to install. Using the feed motor current gives information about the feed force which is duplicated somewhat by the spindle motor current signal. Likewise, power consumption is also directly related to spindle motor current.

Tool Wear

A high quality product often implies high quality surface finish and dimensional accuracy. Ideally, a sharp tool should be maintained at all times. A dull one deforms the surface to a greater depth and may tear the surface which in turn may lower the fatigue resistance. A worn tool also results in more friction which in turn results in higher cutting temperatures. Unwanted effects may arise from these temperatures, e.g. it may produce untempered martensite in heat treatable steel (Schey, 1977). Therefore, tool wear has to be controlled.

Tool wear comes in different forms. Apart from the intuitive rounding of the cutting edge, crater wear on the rake face due to the abrasion of the sliding of the chip on the rake face and flank wear due to friction of the tool on the workpiece occur. Speed of cutting, more than other parameters, influence the rate of wear; depth of cut and feed rate also affect the tool life. In our experiments, we measured the flank wear VB as a generally accepted parameter for evaluating tool wear (Figure 5).

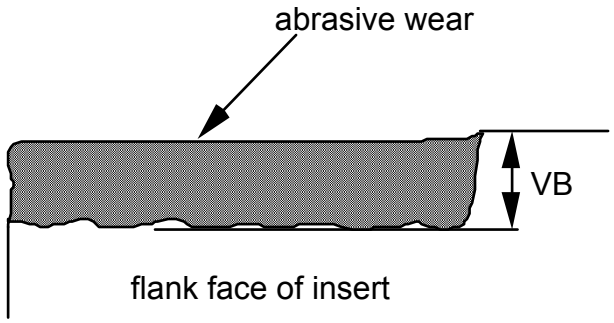

Figure 5 - Tool wear VB as it is seen on the insert

The flank wear VB is measured as the distance from the cutting edge to the end of the abrasive wear on the flank face of the tool. The flank wear was observed during the experiments. The insert was taken out of the tool and the wear was measured with the help of a microscope. The results of one of these experiments is displayed in Figure 6.

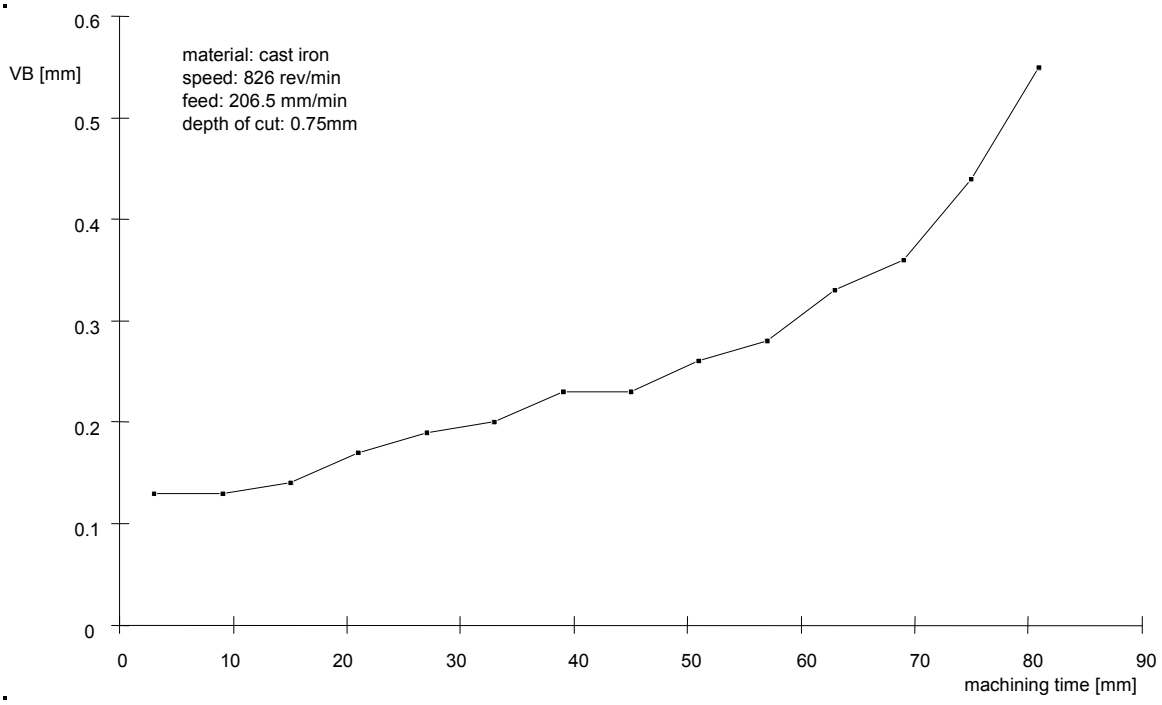

Figure 6 - Tool wear VB over time

Lastly, chipping and fracture are other forms of tool wear caused by discontinuous machining, inclusions in the material, and overloading the tool (Schey, 1977). Mathematical functions for gradual wear try to describe tool wear, for example Taylor's formula:

$$T = C_v v_c^k$$

where:

T = tool life

v_c = cutting speed

k = Taylor exponent

C_V = constant related to 1 min tool life

k and C_V are characteristics of the tool and the workpiece material combination. The limitations of this approach are that different materials and wear due to the influence of feed cannot be accounted for. Apart from that the problem with tool wear in general is that it may not be very predictive; slight variations in a seemingly same setting vary the tool life considerably. These variations are manifold. One is that the same material can have different strengths which is often the case with cast iron. But this variation can also be local in form of inclusions. These can initiate increased wear when they remove large chunks of an insert. Even is the abrasion is of a smaller degree, the geometry of the insert changes, i.e., the insert becomes less sharp and as a result the tool has to plow through the material with greater force, more friction and, as a result, greater tool wear. Other variations are the amount of coolant used to control the temperature of the cutting process. Two thirds of the heat generated during the cutting process is removed via chip and tool. Changing this temperature may have an effect on chemical processes by allowing alloying elements to diffuse into the workpiece and thus weaken the structure of the insert. Furthermore, the depth of cut may not be steady, in particular when machining a new rough surface for the first time. All of these influences may be small, but they can add up over the period of machining to cause considerable uncertainty in predicting a priori the tool life.

The use of additional parameters s^i in Taylor's formula to result in

$$T = C_v v_c^k s^i$$

try to incorporate such influences, however only with modest success. These shortcomings again motivate the use of non-mathematical techniques.

Appendix

The appendix shows some typical signatures from the different sensors

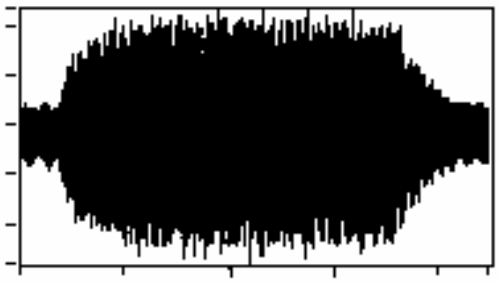

Figure 7 - Spindle motor current (AC)

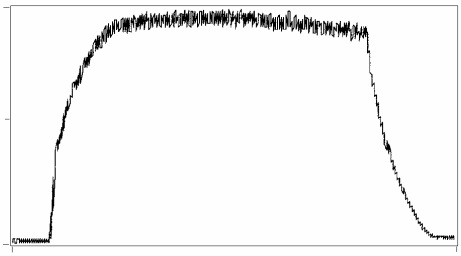

Figure 8 - Spindle motor current (DC portion)

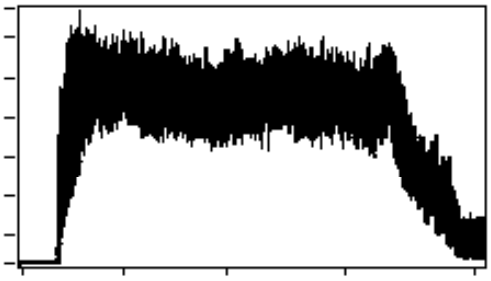

Figure 9 -Acoustic emission (table)

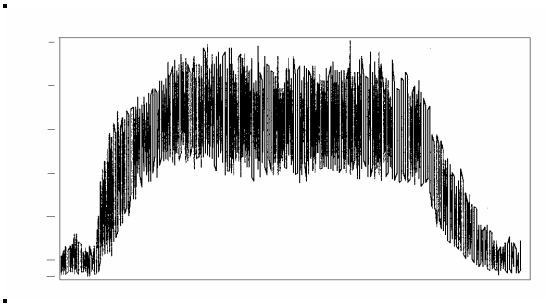

Figure 10 - Acoustic emission (spindle)

Figure 11 - Vibration (table)

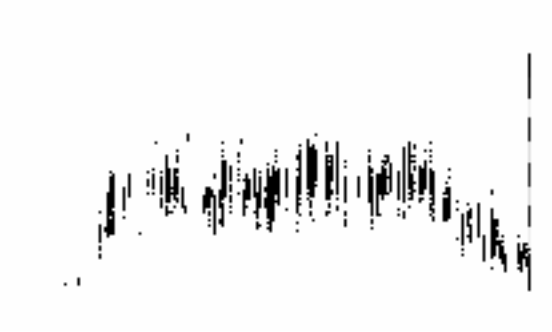

Figure 12 - Vibration (spindle)

References

K. Goebel, Management of Uncertainty in Sensor Validation, Sensor Fusion, and Diagnosis of Mechanical Systems Using Soft Computing Techniques, Ph.D. Thesis, Department of Mechanical Engineering, University of California at Berkeley, 1996.